Adaptive Position and Orientation Regulation for the Camera-in-Hand Problem

Aman Behal*
Electrical and Computer Engineering
Clarkson University
Potsdam, New York 13699-5720
e-mail: abehal@clarkson.edu

P. Setlur
Electrical and Electronic Engineering
California State University at Sacramento
Sacramento, California 95819-6019
e-mail: setlurp@ecs.csus.edu

Warren Dixon
Mechanical and Aerospace Engineering
University of Florida
Gainesville, Florida 32611
e-mail: wdixon@ufl.edu

Darren M. Dawson
Electrical & Computer Engineering
Clemson University
Clemson, South Carolina 29634
e-mail: ddawson@ces.clemson.edu

Received 20 September 2003; accepted 19 May 2005

This paper considers the camera-space position and orientation regulation problem for the camera-in-hand problem via visual serving in the presence of parametric uncertainty associated with the robot dynamics and the camera system. Specifically, an adaptive robot controller is developed that forces the end-effector of a robot manipulator to move such that the position and orientation of an object are regulated to a desired position and ori-

*To whom all correspondence should be addressed.

Journal of Robotic Systems 22(9), 457–473 (2005) © 2005 Wiley Periodicals, Inc.
Published online in Wiley InterScience (www.interscience.wiley.com). • DOI: 10.1002/rob.20079

entation in the camera-space, despite parametric uncertainty throughout the entire robot-camera system. An extension is also provided that illustrates how slight modifications can be made to the camera-in-hand control law to achieve adaptive position and orientation tracking of the end-effector in the camera-space for a fixed-camera configuration. Simulation results are provided to illustrate the performance of the adaptive, camera-in-hand controller. © 2005 Wiley Periodicals, Inc.

1. INTRODUCTION

To achieve high-performance control of a robotic system, it is generally accepted that sensor-based control is required. If the robot is operating in an unstructured environment, an interesting approach is to utilize a vision system for obtaining the position information required by the controller. Hence, the vision system can be used for both on-line trajectory planning and feedforward/feedback control (i.e., visual servoing). In addition, there seems to be a consensus that to extract high-level performance from vision-based robotic systems, the control system must incorporate information about the dynamics/kinematics of the robot and the calibration parameters of the camera system. [The camera calibration parameters are composed of the so-called intrinsic parameters (i.e., image center, camera scale factors, and camera magnification factor) and extrinsic parameters (i.e., camera position and orientation).] As stated in ref. 1, few vision-based controllers have been proposed that take into account the nonlinear robot dynamics. That is, many of the previously developed controllers are designed under that assumption that the robot is a perfect positioning device with negligible dynamics, and hence, reduce the problem to that of kinematic control based on camera observations (e.g., ref. 2). One of the first vision-based control designs which incorporated the robot dynamics can be found in ref. 3; however, the vision system was modeled as a simple rotation transformation. More recently in ref. 4, Bishop et al. emphasized the importance of adequate calibration of the vision system with respect to the robot and the environment. As noted in ref. 4, while a variety of techniques have been proposed for off-line camera calibration, only a few approaches were aimed at the more interesting problem of on-line calibration under closed-loop control. An overview of the state-of-the-art in robot visual servoing can be found in refs. 5 and 6.

Recently, some attention has been given to the design of vision-based controllers that guarantee the convergence of the position error. Specifically, Kelly and Marquez[7] considered a more representative model of the camera-robot system (in comparison to the approach of ref. 3) to design a setpoint controller for the fixed-camera problem that compensated for unknown intrinsic camera parameters but required perfect knowledge of the camera orientation. In ref. 1, Kelly redesigned the setpoint controller of ref. 7 to also take into account uncertainties associated with the camera orientation and produce a local asymptotic stability result; however, the result given in ref. 1 required exact knowledge of the robot gravitational term and that the difference between the estimated and actual camera orientation was restricted to the interval $(-90°, 90°)$. In ref. 8, Kelly et al. utilized a composite velocity inner loop, image-based outer loop fixed-camera position tracking controller to obtain a local asymptotic stability result; however, exact model knowledge of the robot dynamics and a calibrated camera are required, and the difference between the estimated and actual camera orientation is restricted to the interval $(-90°, 90°)$. In ref. 9, Kelly et al. extended the transpose Jacobian control philosophy given in ref. 10 to develop a position regulation controller for the camera-in-hand problem, provided exact knowledge of the gravity of the robot gravitational term is available. In ref. 11, Maruyama and Fujita proposed position setpoint controllers for the camera-in-hand configuration; however, the proposed controllers required exact knowledge of the camera orientation and assumed the camera scaling factors to be the same value for both directions. In ref. 4, Bishop and Spong developed an inverse dynamics-type, position tracking control scheme (i.e., exact model knowledge of the mechanical dynamics) with an on-line adaptive camera calibration control loop that guaranteed asymptotic position tracking; however, convergence of the position tracking error required that the desired position trajectory be persistently exciting. Recently, in ref. 12, Zergeroglu et al. designed an adaptive position tracking controller for a fixed-camera configuration that accounted for parametric uncertainty throughout the entire robot-camera system provided the camera orientation is restricted to the interval $(-90°, 90°)$. Moreover, in ref. 13, Zergeroglu *et al.* proposed (i) a uniformly ultimately bounded (UUB) position tracking controller that rejects uncertainty throughout the entire robot-camera system for a fixed-camera configuration, and

(ii) a UUB regulating controller for a camera-in-hand configuration provided the camera orientation is within a certain range.

In this paper, we extend the work given in refs. 12–14 to develop an adaptive position and orientation regulation controller for the camera-in-hand configuration. Specifically, despite parametric uncertainty in the robot manipulator and the camera system, we force the end-effector to move such that the position and orientation of an object in the camera-space are regulated to a desired position and orientation. An extension is also provided that illustrates how the proposed control strategy can also be utilized to obtain asymptotic position and orientation tracking of the end-effector in the camera-space for the fixed-camera problem. With respect to much of the research presented in the literature, the proposed adaptive robot controller has the following advantages: (i) parametric uncertainty throughout the entire robot/camera system is confronted, and (ii) the position and the orientation of an object are regulated. An additional advantage of the controller proposed in the fixed-camera extension is that the more general position and orientation tracking problem is solved.

The paper is organized in the following manner. Section 2 describes the robot manipulator-camera system model while the control objective, open-loop error system, control design, and closed-loop error system are given in Section 3. A Lyapunov-based stability analysis is provided in Section 4. A position and orientation tracking extension is presented in Section 5 for the fixed-camera problem. Simulation results illustrating the performance of the control law are given in Section 6 and concluding remarks are presented in Section 7.

2. MODEL DEVELOPMENT

2.1. Kinematic Model

To obtain the kinematic equations that relate the task-space end-effector position of a rigid three-link, revolute, planar robot manipulator to the joint displacements, we define a set of task-space variables $x_1(t)$, $x_2(t) \in \mathbb{R}^1$, an open set $S_1 \subset \mathbb{R}^2$, and a function $\Omega \in C^2(S_1)$ where $\Omega: S_1 \to \mathbb{R}^2$, such that

$$[x_1(t) x_2(t)]^T = \Omega(q_1, q_2) \tag{1}$$

where $q_1(t)$, $q_2(t) \in \mathbb{R}^1$ represent the displacements of the first two joints (see Figure 1). After taking the time derivative of (1), we obtain the following expression:

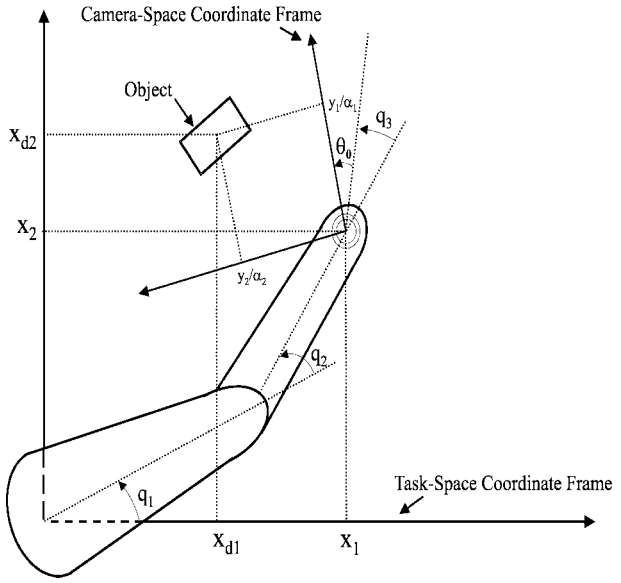

Figure 1. Three-link robot manipulator.

$$[\dot{x}_1(t) \dot{x}_2(t)]^T = J[\dot{q}_1(t) \dot{q}_2(t)]^T \tag{2}$$

where the Jacobian matrix $J(q_1, q_2) \in \mathbb{R}^{2\times 2}$ is defined as

$$J(q_1, q_2) = \left[\frac{\partial \Omega(q_1, q_2)}{\partial q_1} \frac{\partial \Omega(q_1, q_2)}{\partial q_2} \right] \tag{3}$$

where we assume that $J \in C^1(S_1)$. We can also relate the end-effector orientation, denoted by $\theta(t) \in \mathbb{R}^1$, to the joint displacements as shown in the following expression:

$$\theta = q_1 + q_2 + q_3 \tag{4}$$

where $q_3(t) \in \mathbb{R}^1$ represents the displacement of the third joint. After taking the time derivative of (4) and combining the resulting expression with (2), we obtain the following expression:

$$\dot{x} = J_S \dot{q} \tag{5}$$

where $\dot{q}(t)$ represents the time derivative of $q(t) = [q_1(t)\ q_2(t)\ q_3(t)]^T \in \Re^3$, $\dot{x}(t)$ represents the time derivative of $x(t) = [x_1(t)\ x_2(t)\ \theta(t)]^T \in \mathbb{R}^3$, and $J_S(q) \in \mathbb{R}^{3\times 3}$ is defined as follows:

$$J_S = \begin{bmatrix} J & 0_{2\times 1} \\ 1_{1\times 2} & 1 \end{bmatrix}, \tag{6}$$

where $J(q_1, q_2)$ was defined in (3), and the notation $\xi_{n\times m}$ signifies that ξ is an $n \times m$ matrix.

Remark 1: In the previous development, we have assumed that the third link of the manipulator has no length (i.e., the third link does not affect the position of the end-effector, only the orientation of the end-effector) to simplify the control development and stability analysis. Based on the results of this paper, one could easily extend the control design to solve the camera-space position and orientation regulation problem for a rigid three-link manipulator, where each link has some length. In Section 5, we propose an adaptive tracking controller for the fixed-camera problem using a rigid, three-link manipulator where each link has some length.

Remark 2: During the subsequent control development, we assume that $J^{-1}(q)$ always exists and all kinematic singularities are always avoided.

2.2. Task-Space to Camera-Space Transformations

To develop a relationship between the task-space position and orientation of an object and the camera-space position and orientation, we utilize the so-called pin-hole lens model[4] for the robot-camera system that is modified to reflect the properties of the camera-in-hand problem[11] as shown below:

$$\begin{bmatrix} y_1 \\ y_2 \end{bmatrix} = BR(\theta)\left(\begin{bmatrix} x_1 \\ x_2 \end{bmatrix} - \begin{bmatrix} x_{d1} \\ x_{d2} \end{bmatrix}\right) \tag{7}$$

where $y(t) = [y_1(t)\ y_2(t)] \in \mathbb{R}^2$ represents the position of the object in the camera-space, $x_1(t), x_2(t) \in \mathbb{R}^1$ represent the position of the end-effector in the task-space, $B \in \mathbb{R}^{2\times 2}$ is a constant matrix defined as follows:

$$B = AR(\theta_0). \tag{8}$$

$A \in \mathbb{R}^{2\times 2}$ is a diagonal, positive-definite, constant matrix defined as follows:

$$A = \begin{bmatrix} \alpha_1 & 0 \\ 0 & \alpha_2 \end{bmatrix}. \tag{9}$$

$R(\cdot) \in \mathbb{R}^{2\times 2}$ is a rotation matrix operator defined as

$$R(\cdot) = \begin{bmatrix} \cos(\cdot) & \sin(\cdot) \\ -\sin(\cdot) & \cos(\cdot) \end{bmatrix}. \tag{10}$$

$x_d = [x_{d1}\ x_{d2}]^T \in \mathbb{R}^2$ represents the constant, desired task-space position of the object, α_1, $\alpha_2 \in \mathbb{R}^1$ are positive constants defined as

$$\alpha_1 = \beta_1 \frac{\lambda}{z} \quad \alpha_2 = \beta_2 \frac{\lambda}{z}. \tag{11}$$

$z \in \mathbb{R}^1$ represents the constant distance of the camera's optical center to the task-space plane, $\lambda \in \mathbb{R}^1$ is a constant representing the camera's focal length, the positive constants denoted by $\beta_1, \beta_2 \in \mathbb{R}^1$ represent the camera's constant scale factors (in pixels/m) along their respective Cartesian directions, and $\theta_0 \in \mathbb{R}^1$ represents the unknown, constant counter-clockwise rotation angle of the camera. To relate the task-space orientation of the object to the camera-space orientation, we utilize the following relationship (see Appendix A for details regarding the development of the following expression):

$$\tan\theta_y = \frac{\alpha_2}{\alpha_1} \tan[\theta_d - (\theta_0 + \theta)] \triangleq \theta_T, \tag{12}$$

where $\theta_T \in \mathbb{R}^1$ is a measurable auxiliary camera-space signal, $\theta_d \in \mathbb{R}^1$ represents the constant desired orientation of the object in the task-space, $\theta_y(t) \in \mathbb{R}^1$ represents the orientation of the object in the camera-space, and $\theta(t)$ was defined in (4).

Remark 3: In a similar manner as in ref. 13, we assume that the camera is mounted such that (i) its image plane is parallel to the plane of the object, (ii) the camera system can determine the position of an object by locating a feature (e.g., a light emitting diode), (iii) the camera can determine the orientation of the object by recognizing at least one additional feature (e.g., a second light emitting diode, etc.), (iv) the camera can capture images of the object throughout the entire robot workspace, and (v) the effects of image capturing and processing delays are negligible (this assumption is reasonable since advancements in computer and high-speed camera technology provide vision systems with the capability to capture frames, process the data, and compute the controller within a millisecond). Moreover, we must assume that the initial orientation error is restricted as follows:

$$|\theta_T(0)| < 90\,[\text{deg}] \tag{13}$$

where $\theta_T(t)$ was defined in (12).

2.3. Joint-Space to Camera-Space Transformations

To relate the joint-space signals to the camera-space signals, we first take the time derivative of the expressions given in (7) and (12) and then perform some algebraic manipulation to obtain the following expressions:

$$\begin{bmatrix}\dot{y}_1\\ \dot{y}_2\end{bmatrix} = BJ_2R(\theta)\left(\begin{bmatrix}x_1\\ x_2\end{bmatrix} - \begin{bmatrix}x_{d1}\\ x_{d2}\end{bmatrix}\right)\dot{\theta} + BR(\theta)J\begin{bmatrix}\dot{q}_1\\ \dot{q}_2\end{bmatrix},$$

$$\dot{\theta}_T = -\gamma\dot{\theta} \tag{14}$$

where $J_2 \in \mathbb{R}^{2\times 2}$ is a skew-symmetric matrix defined as follows:

$$J_2 = \begin{bmatrix}0 & 1\\ -1 & 0\end{bmatrix} \tag{15}$$

and $\gamma(q) \in \mathbb{R}^1$ is a positive scalar function defined as

$$\gamma = \frac{(1+\theta_T^2)}{\frac{\alpha_1}{\alpha_2}\cos^2[\theta_d - (\theta_0+\theta)] + \frac{\alpha_2}{\alpha_1}\sin^2[\theta_d - (\theta_0+\theta)]}. \tag{16}$$

After utilizing (7) and (14), we obtain the following transformation between the joint-space and the camera-space

$$\dot{Y} = TC\dot{q}, \quad \dot{q} = C^{-1}T^{-1}\dot{Y} \tag{17}$$

where $Y(t) \in \mathbb{R}^3$ is defined as

$$Y(t) = [y^T(t)\ \theta_T(t)]^T \tag{18}$$

and $T(q,y)$, $C(q) \in \mathbb{R}^{3\times 3}$ are global invertible transformations defined as

$$T = \begin{bmatrix}B & BJ_2B^{-1}y\\ 0_{1\times 2} & -\gamma\end{bmatrix} \tag{19}$$

and

$$C = \begin{bmatrix}R(\theta)J & 0_{2\times 1}\\ 1_{1\times 2} & 1\end{bmatrix}, \tag{20}$$

respectively, where $B \in \mathbb{R}^{2\times 2}$ was defined in (8), $\gamma(q)$ was defined in (16), $J(q)$ was defined in (2), and $R(\cdot)$ was defined in (10). Note that the inverse of C is guaranteed to exist based on the assumption that the inverse of the Jacobian matrix $J(q)$ exists (see Remark 2). Furthermore, the inverse of $T(q,y)$ can be written in the following form:

$$T^{-1} = \begin{bmatrix}D & 0_{2\times 1}\\ H & -\frac{1}{\gamma}\end{bmatrix}^T \tag{21}$$

where $D \in \mathbb{R}^{2\times 2}$ and $H \in \mathbb{R}^{1\times 2}$ are defined as follows:

$$D \triangleq \begin{bmatrix}d_1 & d_2\\ d_3 & d_4\end{bmatrix} = \begin{bmatrix}\frac{\cos\theta_0}{\alpha_1} & \frac{\sin\theta_0}{\alpha_1}\\ -\frac{\sin\theta_0}{\alpha_2} & \frac{\cos\theta_0}{\alpha_2}\end{bmatrix}, \tag{22}$$

$$H = \frac{\alpha_1^2\cos^2[\theta_d - (\theta_0+\theta)] + \alpha_2^2\sin^2[\theta_d - (\theta_0+\theta)]}{(1+\theta_T^2)\alpha_2^2\alpha_1^2} \times \begin{bmatrix}\alpha_2 y_1\sin\theta_0 + \alpha_1 y_2\cos\theta_0\\ -\alpha_2 y_1\cos\theta_0 + \alpha_1 y_2\sin\theta_0\end{bmatrix}^T. \tag{23}$$

2.4. Dynamic Model

The joint-space dynamic model for a rigid three-link, revolute, planar robot manipulator is assumed to have the following form:[15]

$$M(q)\ddot{q} + V_m(q,\dot{q})\dot{q} + G(q) + F(\dot{q}) = \tau \tag{24}$$

where $q(t)$, $\dot{q}(t)$, $\ddot{q}(t) \in \mathbb{R}^3$ denote the link position, velocity, and acceleration vectors, respectively, $M(q) \in \mathbb{R}^{3\times 3}$ represents the inertia matrix, $V_m(q,\dot{q}) \in \mathbb{R}^{3\times 3}$ represents the centripetal-Coriolis matrix, $G(q) \in \mathbb{R}^3$ represents the gravity effects, $F(\dot{q}) \in \mathbb{R}^3$ represents the friction effects, and $\tau(t) \in \mathbb{R}^3$ is the torque input vector. To facilitate the subsequent control design and stability analysis, we transform the dynamic model into a form that is consistent with the camera-space transformations given by (14) and (17). Specifically, we premultiply (24) by the product

$T^{-T}(q,y)C^{-T}(q)$ and then substitute (17) into (24) for $\dot{q}(t)$ to obtain the following expression:

$$M^*(q,Y)\ddot{Y} + V_m^*(q,\dot{q},Y,\dot{Y})\dot{Y} + G^*(q,Y) + F^*(q,\dot{q},Y) = T^{-T}\tau^* \tag{25}$$

where

$$M^*(q,Y) = T^{-T}C^{-T}M(q)C^{-1}T^{-1},$$

$$V_m^*(q,\dot{q},Y,\dot{Y}) = T^{-T}C^{-T}[M(q)(C^{-1}\dot{T}^{-1} + \dot{C}^{-1}T^{-1}) + V_m(q,\dot{q})C^{-1}T^{-1}],$$

$$G^*(q,Y) = T^{-T}C^{-T}G(q),$$

$$F^*(q,\dot{q},Y) = T^{-T}C^{-T}F(\dot{q}),$$

$$\tau^*(q,t) = C^{-T}\tau, \tag{26}$$

and the notation $(\cdot)^{-1}$ signifies the time derivative of $(\cdot)^{-1}$. In the subsequent control development and stability analysis, we will exploit the following properties[16] of the expressions given in (16) and (21), and the dynamic model given in (25) and (26).

Property 1: The transformed inertia matrix $M^*(\cdot)$ is symmetric, positive definite, and satisfies the following inequalities:

$$m_1\|\xi\|^2 \leqslant \xi^T M^* \xi \leqslant m_2\|\xi\|^2, \quad \forall\, \xi \in \mathbb{R}^3 \tag{27}$$

where m_1 and m_2 are known positive constants, and $\|\cdot\|$ denotes the standard Euclidean norm.

Property 2: A skew-symmetric relationship exists between the transformed inertia matrix and the auxiliary matrix $V_m^*(\cdot)$ as follows:

$$\xi^T\left(\frac{1}{2}\dot{M}^* - V_m^*\right)\xi = 0, \quad \forall\, \xi \in \mathbb{R}^3 \tag{28}$$

where $\dot{M}^*(\cdot)$ represents the time derivative of the transformed inertia matrix.

Property 3: The robot dynamics given in (25) can be linearly parametrized as follows:

$$Y_0\vartheta_0 = M^*\ddot{Y} + V_m^*\dot{Y} + G^* + F^* \tag{29}$$

where $\vartheta_0 \in \mathbb{R}^p$ contains the unknown constant mechanical parameters (i.e., inertia, mass, and friction effects) and the constant camera calibration constants (i.e., θ_0, α_1, and α_2) and $Y_0(Y,\dot{Y},\ddot{Y}) \in \mathbb{R}^{3\times p}$ denotes a known regression matrix. The inverse of the auxiliary signal $\gamma(q)$ defined in (16) can also be linearly parametrized as shown below:

$$\frac{1}{\gamma} = Y_\gamma\phi_\gamma > \rho \tag{30}$$

where $\rho \in \mathbb{R}^1$ is a positive bounding constant, $\phi_\gamma \in \mathbb{R}^{p2}$ contains the constant camera calibration constants (i.e., θ_0, α_1, and α_2), and $Y_\gamma(q) \in \mathbb{R}^{1\times p2}$ denotes a known regression matrix.

Property 4: To avoid singularities in the subsequent control law, we now define convex a region, in the same manner as refs. 14 and 17, for the parameter vector ϕ_γ defined in (30). Specifically, based on (30), we define the space spanned by the vector function $Y_\gamma(q)$ as follows:

$$Y_1 = \{Y_\gamma : Y_\gamma = Y_\gamma(\theta), \quad \forall\, \theta \in \mathbb{R}^1\}. \tag{31}$$

In addition, we define the region Λ_1 as

$$\Lambda_1 = \{s_1 : Y_\gamma s_1 \geqslant \rho, \quad \forall\, Y_\gamma \in Y_1\} \tag{32}$$

where ρ was defined in (30). Moreover, we introduce the following definitions concerning the region Λ_1 and the subsequently designed parameter estimate vector $\hat{\phi}_\gamma(t) \in \mathbb{R}^{p2}$: int($\Lambda_1$) is the interior of the region Λ_1, $\partial(\Lambda_1)$ is the boundary for the region Λ_1, $\hat{\phi}_\gamma^\perp \in \mathbb{R}^{p2}$ is a unit vector normal to $\partial(\Lambda_1)$ at the point of intersection of the boundary surface $\partial(\Lambda_1)$ and $\hat{\phi}_\gamma$ where the positive direction for $\hat{\phi}_\gamma^\perp$ is defined as pointing away from int(Λ_1) [note, $\hat{\phi}_\gamma^\perp$ is only defined for $\hat{\phi}_\gamma \in \partial(\Lambda_1)$], $P_r^t(\mu_1)$ is the component of the vector $\mu_1 \in \mathbb{R}^{p2}$ that is tangential to $\partial(\Lambda_1)$ at the point of intersection of the boundary surface $\partial(\Lambda_1)$ and the vector $\hat{\phi}_\gamma$, and $P_r^\perp(\mu_1) = \mu_1 - P_r^t(\mu_1) \in \mathbb{R}^{p2}$ is the component of the vector $\mu_1 \in \mathbb{R}^{p2}$ that is perpendicular to $\partial(\Lambda_1)$ at the point of intersection of the boundary surface $\partial(\Lambda_1)$ and the vector $\hat{\phi}_\gamma$.

Property 5: We assume that the constant system parameters d_i defined in (22) can be lower and upper bounded as follows:

$$\underline{d}_i < d_i < \bar{d}_i \tag{33}$$

where $\underline{d}_i, \bar{d}_i \in \mathbb{R}^1$ denote known, constant bounds for the unknown parameter d_i for $i=1,2,3,4$.

Remark 4: Since the robot manipulator is solely constructed of revolute joints, the kinematic and dynamic terms denoted by $M(q)$, $V_m(q,\dot{q})$, $G(q)$, $F(\dot{q})$, and $J(q)$ are bounded for all possible $q(t)$ [i.e., these kinematic and dynamic terms only depend on $q(t)$ as arguments of trigonometric functions].

Remark 5: The control laws developed in the subsequent sections will be designed in the camera-space, where the actual control inputs to the robot actuators are computed according to (26); hence, implementation of the proposed control laws will require $q(t)$. Since the camera is assumed to be uncalibrated (i.e., the camera parameters are not known exactly), $q(t)$ cannot be directly calculated from measurements of $y(t)$ and must be measured directly via standard link encoder sensors. The need to measure the joint position from the joint encoders may lead some readers to question why one could not simply utilize link sensors (e.g., optical encoders) to close the loop and only utilize the camera system for trajectory planning. This question seems well motivated, since link sensors are also required to implement vision-based controllers and in comparison with a vision system, link sensors are generally less complex, less costly, and can be used at faster sampling times. However, if the desired camera-space position and orientation are formulated in the camera-space, then it is not obvious how to calculate the desired task-space position and orientation because the camera parameters in (7) and (12) are not exactly known. Hence, a reasonable technique for addressing the uncalibrated camera problem is to develop a control strategy that servos off the difference between the desired position and orientation in the camera space and the actual position and orientation in the camera space.

3. CONTROL DEVELOPMENT

Our control objective is to design a controller that ensures position and orientation regulation of an object in the camera-space for the camera-in-hand configuration. That is, with an uncalibrated camera mounted directly on the end-effector of a robot manipulator with parametric uncertainty, our goal is to design a controller that regulates the robot end-effector such that the camera-space position and orientation of an object are regulated to a constant, desired position and orientation. Based on the control objective and the subsequent control development and stability analysis, we define a filtered error signal,[16] denoted by $r(t)=[r_1\ r_2\ r_3]^T \in \mathbb{R}^3$, as follows:

$$r = \dot{Y} + \mu_r Y \tag{34}$$

where μ_r denotes a positive, constant control gain and $Y(t)$ was defined in (18). Since we will utilize the filtered error signal defined in (34) in the subsequent control design, it is clear that in addition to the required measurement of the link positions in the task-space (as described in Remark 5), we also require measurement of the object orientation, the angular velocity of the object, the position of the object, and the time-derivative of the object position in the camera-space.

Remark 6: Note that for simplicity and without loss of generality, we have selected the desired camera-space position as the origin of the camera-space and the desired orientation as zero degrees.

3.1. Open-Loop Error System

To obtain the open-loop error system for $r(t)$, we take the time derivative of (34), premultiply the resulting expression by $M^*(\cdot)$, and then substitute (25) into the resulting expression for $M^*(\cdot)\ddot{Y}$ to obtain the following expression:

$$M^*\dot{r} = -V_m^*\dot{Y} - G^* - F^* + T^{-T}\tau^* + \mu_r M^*\dot{Y}. \tag{35}$$

After adding and subtracting the products $Y_r(\cdot)\hat{\phi}_r(t)$ and $k_s r(t)$ to the right-side of (35) and then utilizing (34), we can rewrite the open-loop dynamics as follows:

$$M^*\dot{r} = -k_s r - V_m^* r + Y_r\tilde{\phi}_r + Y_r\hat{\phi}_r + k_s r + T^{-T}\tau^* \tag{36}$$

where $k_s \in \mathbb{R}^1$ is a positive constant control gain, the regression matrix parametrization $Y_r\phi_r$ is defined as

$$Y_r\phi_r = \mu_r V_m^* Y - G^* - F^* + \mu_r M^*\dot{Y}. \tag{37}$$

$Y_r(\cdot) \in \mathbb{R}^{3\times r_1}$ denotes a known regression matrix, $\phi_r \in \mathbb{R}^{r_1}$ contains the unknown constant mechanical parameters (i.e., inertia, mass, and friction effects) and camera calibration constants (i.e., θ_0, α_1, and α_2), and

$\tilde{\phi}_r(t) \in \mathbb{R}^{r1}$ denotes a parameter estimation error and is defined as follows:

$$\tilde{\phi}_r(t) = \phi_r - \hat{\phi}_r(t) \tag{38}$$

where $\hat{\phi}_r(t) \in \mathbb{R}^{r1}$ denotes a subsequently designed parameter estimate vector for ϕ_r.

3.2. Closed-Loop Error System

To facilitate the subsequent control design, we define the following linear parametrization:

$$Y_H \phi_H = -H\left(\hat{D}^{-1}\begin{bmatrix}(Y_r\hat{\phi}_r + k_s r)_1 \\ (Y_r\hat{\phi}_r + k_s r)_2\end{bmatrix}\right) \tag{39}$$

where $(\xi)_i$ represents the ith element of a vector ξ, $Y_H(t) \in \mathbb{R}^{1\times p1}$ represents a known regression matrix, $\phi_H \in \mathbb{R}^{p1}$ represents a vector of constant unknown camera calibration parameters, H was defined in (23), $\hat{D}^{-1}(t)$ represents the inverse of $\hat{D}(t) \in \mathbb{R}^{2\times 2}$, a matrix of dynamic estimates for the elements of D, denoted by

$$\hat{D} = \begin{bmatrix}\hat{d}_1 & \hat{d}_2 \\ \hat{d}_3 & \hat{d}_4\end{bmatrix} \tag{40}$$

where $\hat{d}_i(t)$ for $i=1,2,3,4$ are subsequently designed adaptation laws, and $\hat{\phi}_r(t)$ was given in (38). Based on the previous development, we can now develop an adaptive control law to regulate the camera-space position and orientation of an object. Specifically, based on the open-loop error system given in (36) and the subsequent stability proof, we now design the auxiliary control signal $\tau^*(t)$ as follows:

$$\tau^* = \begin{bmatrix}\tau_1^* \\ \tau_2^* \\ \tau_3^*\end{bmatrix} = \begin{bmatrix} -\hat{D}^{-1}\begin{bmatrix}(Y_r\hat{\phi}_r + k_s r)_1 \\ (Y_r\hat{\phi}_r + k_s r)_2\end{bmatrix} \\ \dfrac{1}{Y_\gamma\hat{\phi}_\gamma}[(Y_r\hat{\phi}_r + k_s r)_3 + Y_H\hat{\phi}_H]\end{bmatrix} \tag{41}$$

where the elements of the adaptive estimate matrix $\hat{D}(t)$ given in (40) [i.e., $\hat{d}_i(t)$ for $i=1,2,3,4$] are generated by the following dynamic expressions:

$$\dot{\hat{d}}_i = \begin{cases}\text{Proj}\left\{-\Gamma_i r_1\left(\hat{D}^{-1}\begin{bmatrix}(Y_r\hat{\phi}_r + k_s r)_1 \\ (Y_r\hat{\phi}_r + k_s r)_2\end{bmatrix}\right)_i\right\} & \forall i = 1,2 \\ \text{Proj}\left\{-\Gamma_i r_2\left(\hat{D}^{-1}\begin{bmatrix}(Y_r\hat{\phi}_r + k_s r)_1 \\ (Y_r\hat{\phi}_r + k_s r)_2\end{bmatrix}\right)_{i-2}\right\} & \forall i = 3,4\end{cases} \tag{42}$$

and the parameter estimate $\hat{\phi}_\gamma(t) \in \mathbb{R}^{p2}$ is defined by the following expression:

$$\dot{\hat{\phi}}_\gamma = \begin{cases}\Omega_1 & \text{if } \hat{\phi}_\gamma \in \text{int}(\Lambda_1) \\ \Omega_1 & \text{if } \hat{\phi}_\gamma \in \partial(\Lambda_1) \text{ and } \Omega_1^T\hat{\phi}_\gamma^\perp \leqslant 0 \\ P_r^t(\Omega_1) & \text{if } \hat{\phi}_\gamma \in \partial(\Lambda_1) \text{ and } \Omega_1^T\hat{\phi}_\gamma^\perp > 0\end{cases} \tag{43}$$

where $\hat{\phi}_\gamma(0) \in \text{int}(\Lambda_1)$, the auxiliary signal $\Omega_1(t) \in \Re^{p2}$ is defined as follows:

$$\Omega_1 = -r_3\Gamma_5\frac{Y_\gamma^T}{Y_\gamma\hat{\phi}_\gamma}[(Y_r\hat{\phi}_r + k_s r)_3 + Y_H\hat{\phi}_H] \tag{44}$$

the dynamic estimates $\hat{\phi}_H(t) \in \mathbb{R}^{p1}$ and $\hat{\phi}_r(t) \in \mathbb{R}^{r1}$ are updated according to the following expressions:

$$\dot{\hat{\phi}}_H = r_3\Gamma_6 Y_H^T, \tag{45}$$

$$\dot{\hat{\phi}}_r = \Gamma_7 Y_r^T r, \tag{46}$$

where $\Gamma_i \in \mathbb{R}^1$ for $i=1,2,3,4$ are positive, constant adaptation gain parameters, $\Gamma_5 \in \mathbb{R}^{p2\times p2}$, $\Gamma_6 \in \mathbb{R}^{p1\times p1}$, and $\Gamma_7 \in \mathbb{R}^{r1\times r1}$ are positive, constant diagonal adaptation gain matrices, and the projection operator denoted by Proj{·} is utilized to ensure that the parameter estimates $\hat{d}_i(t)$ for $i=1,2,3,4$ stay within the known region prescribed by (33), and that

$$\hat{d}_1 > |\bar{d}_2|, \quad \hat{d}_4 > |\bar{d}_3|. \tag{47}$$

If $\hat{\phi}_\gamma(0) \in \text{int}(\Lambda_1)$, the above update law for $\hat{\phi}_\gamma(t)$ defined in (43) ensures that $Y_\gamma\hat{\phi}_\gamma > \rho$ (the reader is referred to the definitions given in Property 4, and the explanations given in refs. 14 and 17). After substi-

tuting (41) into (36) for $\tau^*(t)$ and then simplifying the resulting expression, we obtain the final expression for the closed-loop error dynamics for $r(t)$ as follows:

$$M^*\dot{r} = -k_s r - V_m^* r + Y_r\tilde{\phi}_r + \begin{bmatrix} 0 \\ 0 \\ Y_H\tilde{\phi}_H \end{bmatrix} - \begin{bmatrix} \tilde{D}\hat{D}^{-1} & 0_{2\times 1} \\ 0_{1\times 2} & \dfrac{Y_\gamma\tilde{\phi}_\gamma}{Y_\gamma\hat{\phi}_\gamma} \end{bmatrix} \times \begin{bmatrix} (Y_r\hat{\phi}_r + k_s r)_1 \\ (Y_r\hat{\phi}_r + k_s r)_2 \\ [(Y_r\hat{\phi}_r + k_s r)_3 + Y_H\hat{\phi}_H] \end{bmatrix} \tag{48}$$

where the parameter estimation error signals, denoted by $\tilde{D}(t) \in \mathbb{R}^{2\times 2}$, $\tilde{\phi}_\gamma(t) \in \mathbb{R}^{p2}$, $\tilde{\phi}_H(t) \in \mathbb{R}^{p1}$, are defined as follows:

$$\tilde{D} = D - \hat{D} = \begin{bmatrix} \tilde{d}_1 & \tilde{d}_2 \\ \tilde{d}_3 & \tilde{d}_4 \end{bmatrix}, \quad \tilde{\phi}_\gamma = \phi_\gamma - \hat{\phi}_\gamma,$$

$$\tilde{\phi}_H = \phi_H - \hat{\phi}_H. \tag{49}$$

Remark 7: To ensure that the inequalities given in (47) are valid, we must ensure that

$$\underline{d}_1 > |\bar{d}_2| \quad \underline{d}_4 > |\bar{d}_3|. \tag{50}$$

One method to ensure that (50) is valid is to restrict the initial orientation of the camera to the following region:

$$|\theta_0| < 45\ [\text{deg}]. \tag{51}$$

Note that (51) is a sufficient condition, and hence, other conditions may be employed which lead to less conservative bounds on θ_0.

4. STABILITY ANALYSIS

Based on the closed-loop error system given in (48), we can now examine the stability of the adaptive controller developed in the previous section through the following theorem.

Theorem 1: *Provided the assumptions given in Remark 2, Remark 3, and Remark 7 are valid, the control torque input given in* (41)–(43), (45), *and* (46) *ensures that the camera-space position and orientation errors are asymptotically regulated in the sense that*

$$\lim_{t\to\infty} y(t), \theta_y(t) = 0 \tag{52}$$

where $y(t)$ *and* $\theta_y(t)$ *are defined in* (7) and (12).

Proof: To prove Theorem 1, we define a nonnegative function denoted by $V(t) \in \mathbb{R}^1$ as follows:

$$V = \frac{1}{2} r^T M^* r + \frac{1}{2}\sum_{i=1}^{4} \tilde{d}_i\Gamma_i^{-1}\tilde{d}_i + \frac{1}{2}\tilde{\phi}_\gamma^T\Gamma_5^{-1}\tilde{\phi}_\gamma + \frac{1}{2}\tilde{\phi}_H^T\Gamma_6^{-1}\tilde{\phi}_H + \frac{1}{2}\tilde{\phi}_r^T\Gamma_7^{-1}\tilde{\phi}_r. \tag{53}$$

After taking the time derivative of (53) and then substituting (48) into the resulting expression for the product $M^*\dot{r}(t)$, we obtain the following expression:

$$\dot{V} = -k_s r^T r + r^T Y_r\tilde{\phi}_r + r_3 Y_H\tilde{\phi}_H + r^T \begin{bmatrix} -\tilde{D}\hat{D}^{-1} & 0_{2\times 1} \\ 0_{1\times 2} & -\dfrac{Y_\gamma\tilde{\phi}_\gamma}{Y_\gamma\hat{\phi}_\gamma} \end{bmatrix} \times \begin{bmatrix} (Y_r\hat{\phi}_r + k_s r)_1 \\ (Y_r\hat{\phi}_r + k_s r)_2 \\ [(Y_r\hat{\phi}_r + k_s r)_3 + Y_H\hat{\phi}_H] \end{bmatrix} - \sum_{i=1}^{4} \tilde{d}_i\Gamma_i^{-1}\dot{\hat{d}}_i - \tilde{\phi}_\gamma^T\Gamma_5^{-1}\dot{\hat{\phi}}_\gamma - \tilde{\phi}_H^T\Gamma_6^{-1}\dot{\hat{\phi}}_H - \tilde{\phi}_r^T\Gamma_7^{-1}\dot{\hat{\phi}}_r \tag{54}$$

where we utilized (28) and the facts that

$$\dot{\tilde{\phi}}_r(t) = -\dot{\hat{\phi}}_r(t), \quad \dot{\tilde{\phi}}_\gamma(t) = -\dot{\hat{\phi}}_\gamma(t),$$

$$\dot{\tilde{\phi}}_H(t) = -\dot{\hat{\phi}}_H(t), \quad \dot{\tilde{d}}_i(t) = -\dot{\hat{d}}_i(t), \quad \forall\, i = 1,2,3,4. \tag{55}$$

After utilizing (42)–(46), and the development given in Appendix B, we obtain the following expression:

$$\dot{V} \leq -k_s r^T r \tag{56}$$

hence, utilizing (53) and (56), we can prove that $r(t)$, $\tilde{\phi}_r(t)$, $\tilde{\phi}_\gamma(t)$, $\tilde{\phi}_H$, $\tilde{d}_i \in \mathcal{L}_\infty$ for $i=1,2,3,4$ and that $r(t) \in \mathcal{L}_2$. Since $\tilde{\phi}_r(t)$, $\tilde{\phi}_\gamma(t)$, $\tilde{\phi}_H$, $\tilde{d}_i \in \mathcal{L}_\infty$ for $i=1,2,3,4$, it is clear from (38) and (49) that $\hat{\phi}_r(t)$, $\hat{\phi}_\gamma(t)$, $\hat{\phi}_H$, $\hat{d}_i \in \mathcal{L}_\infty$ for

$i=1,2,3,4$. Based on the fact that $r(t) \in \mathcal{L}_\infty$, we can utilize (18) and (34) to prove that $Y(t)$, $\dot{Y}(t)$, $y(t)$, $\dot{y}(t)$, $\theta_T(t)$, $\dot{\theta}_T(t) \in \mathcal{L}_\infty$. Using the facts that $y(t)$, $\theta_T(t)$, $\dot{\theta}_T(t) \in \mathcal{L}_\infty$, we can utilize (7)–(9), (12), (14), (16), and (10) to prove that $x_1(t)$, $x_2(t)$, $\theta(t)$, $\dot{\theta}(t)$, $\gamma(q) \in \mathcal{L}_\infty$. Based on the previous boundedness arguments and the definitions given in (8)–(10) and (19)–(23), it is clear that $T(q,y)$, $T^{-1}(q,y)$, $C(q)$, $C^{-1}(q) \in \mathcal{L}_\infty$, and hence, from (26) and Remark 4, it is clear that $M^*(q,Y), V_m^*(q,\dot{q},Y,\dot{Y}), G^*(q,Y), F^*(q,\dot{q},Y) \in \mathcal{L}_\infty$. Based on the previous boundedness arguments, we can utilize (30), (37), and (39) to prove that $Y_\gamma(\cdot)$, $Y_H(\cdot)$, $Y_r(\cdot) \in \mathcal{L}_\infty$. Using the fact that $r(t)$, $Y_\gamma(\cdot)$, $Y_H(\cdot)$, $Y_r(\cdot) \in \mathcal{L}_\infty$, we can conclude from (41)–(43), (45), and (46) that $\tau^*(t) \in \mathcal{L}_\infty$, where we have utilized the fact that the adaptive update laws given in (42) and (43) are designed to ensure that potential singularities in (41) are always avoided. Based on the facts that $\tau^*(t) \in \mathcal{L}_\infty$ and $C(q)$ are invertible (based on the assumption that the kinematic singularities are always avoided [(i.e., $J^{-1}(q)$ exists)]), we can utilize (26) to prove that $\tau(t) \in \mathcal{L}_\infty$. Since $r(t)$, $Y_r(q)$, $\tilde{\phi}_r(t)$, $Y_H(t)$, $\tilde{\phi}_H(t)$, $\tilde{d}_i(t)$, $\hat{d}_i^{-1}(t) \in \mathcal{L}_\infty$ for $i=1,2,3,4$, we can utilize (36) to prove that $\dot{r}(t) \in \mathcal{L}_\infty$. Based on the fact that $r(t)$, $\dot{r}(t)$, $Y(t)$, $\dot{Y}(t) \in \mathcal{L}_\infty$, it is clear that $r(t)$ and $Y(t)$ are uniformly continuous. After taking the time derivative of (34) and utilizing the facts that $\dot{r}(t)$, $\dot{Y}(t) \in \mathcal{L}_\infty$, we can also prove that $\ddot{Y}(t) \in \mathcal{L}_\infty$, and hence $\dot{Y}(t)$ is uniformly continuous.

From the fact that $r(t) \in \mathcal{L}_2$, we can prove that $Y(t)$, $\dot{Y}(t) \in \mathcal{L}_2$ (see the proof of Lemma 1.6 of ref. 18). Based on the facts that $r(t)$, $Y(t)$, and $\dot{Y}(t) \in \mathcal{L}_2$ are all uniformly continuous, we can now employ a corollary to Barbalat's Lemma[19] to conclude that

$$\lim_{t\to\infty} r(t), Y(t), \dot{Y}(t) = 0 \tag{57}$$

and hence, from (18), it is straightforward that

$$\lim_{t\to\infty} y(t), \theta_T(t) = 0. \tag{58}$$

Based on the fact that $\theta_T(t) \in \mathcal{L}_\infty$, we can utilize (12), (13), and (58) to prove the result given in (52). □

5. FIXED CAMERA EXTENSION

In this section, we illustrate how the development given in the previous sections can be slightly modified to achieve position and orientation tracking of the end-effector of a rigid three-link manipulator in the camera-space, for an uncalibrated fixed-camera. Specifically, with an uncalibrated camera that is fixed in a constant position that allows the camera to view the entire workspace, we illustrate that for the position and orientation of the end-effector, a rigid three-link manipulator (each link having some length) with uncertain mechanical parameters can track a time-varying trajectory designed in the camera space.

5.1. Model Development

Based on the fact that the camera is fixed at a constant position parallel with the workspace plane, rather than in the camera-in-hand configuration, we must reexamine the camera model. To this end, we utilize the pinhole lens model[20] for the fixed camera to modify (7) as shown below:

$$\begin{bmatrix} y_1 \\ y_2 \end{bmatrix} = AR(\theta_0) \begin{bmatrix} x_1 \\ x_2 \end{bmatrix} + p \tag{59}$$

where $p \in \mathbb{R}^2$ is a constant vector containing unknown camera parameters as shown below:

$$p = \begin{bmatrix} O_{i1} \\ O_{i2} \end{bmatrix} - AR(\theta_0) \begin{bmatrix} O_{o1} \\ O_{o2} \end{bmatrix} \tag{60}$$

where A was defined in (9), $R(\cdot)$ was defined in (10), $[O_{o1}, O_{o2}]^T \in \mathbb{R}^2$ denote the projection of the camera's optical center on the (X_1, X_2) plane, and $[O_{i1}, O_{i2}]^T \in \mathbb{R}^2$ denote the image center that is defined as the frame buffer coordinates of the intersection of the optical axis with the image plane (see ref. 20 for details).

5.2. Open-Loop Error System

The control objective in this extension is to force the end-effector of a rigid, three-link revolute robot manipulator to move such that the position and orientation of the image of the end-effector in the camera-space is forced to track a desired time-varying camera-space trajectory. To quantify the control objective, we define a position and orientation filtered tracking error signal $r(t)=[r_1 r_2 r_3]^T \in \mathbb{R}^3$, as follows:

$$r = \dot{e} + \mu_r e \tag{61}$$

where μ_r was defined in (34) and $e(t) \in \mathbb{R}^3$ is defined as follows:

$$e = Y_d - Y. \tag{62}$$

$Y(t)$ was defined in (18), $y(t) \in \mathbb{R}^2$ was defined in (59), and $\theta_T(t) \in \mathbb{R}^1$ given in (12) is redefined as follows (see Appendix A for details regarding the development of the following expression):

$$\tan \theta_y = \frac{\alpha_2}{\alpha_1} \tan(\theta - \theta_0) \triangleq \theta_T \tag{63}$$

and $Y_d(t) \in \mathbb{R}^3$ is a desired position and orientation vector defined as follows:

$$Y_d = [y_{d1} \quad y_{d2} \quad y_{d3}]^T$$

where $y_{d1}(t)$, $y_{d2}(t) \in \mathbb{R}^1$ represent the desired position of the end-effector in the camera-space and $y_{d3}(t) \in \mathbb{R}^1$ denotes the desired orientation of the end-effector in the camera-space.

After taking the time derivative of (59) and (63), we obtain the following expression:

$$\dot{Y} = TC\dot{q}, \quad \dot{q} = C^{-1}T^{-1}\dot{Y}$$

where $q(t)$ was defined in (5), the matrices $T(q,y)$ and $C(q)$ originally given in (17) are redefined as

$$T = \begin{bmatrix} AR(\theta_0) & 0_{2\times 1} \\ 0_{1\times 2} & \gamma \end{bmatrix} \tag{64}$$

and

$$C = \begin{bmatrix} J_{2\times 3} \\ 1_{1\times 3} \end{bmatrix} \tag{65}$$

where $\gamma(q)$ is redefined as

$$\gamma = \frac{(1 + \theta_T^2)}{\frac{\alpha_1}{\alpha_2}\cos^2(\theta - \theta_0) + \frac{\alpha_2}{\alpha_1}\sin^2(\theta - \theta_0)}.$$

$\dot{Y}_d(t)$ represents the time derivative of the $Y_d(t)$ given in (62), the Jacobian defined in (6) is now defined as a 2×3 matrix as shown in (65), the inverse of $C(q)$ is assumed to exist, and the inverse of $T(q,y)$ is given by the following expression:

$$T^{-1} = \begin{bmatrix} D & 0_{2\times 1} \\ 0_{1\times 2} & \dfrac{1}{\gamma} \end{bmatrix}^T \tag{66}$$

where the submatrix D was defined in (22).

We can now obtain a relationship between the camera-space and the joint-space as follows:

$$\dot{q} = C^{-1}T^{-1}(\dot{Y}_d - \dot{e}). \tag{67}$$

Utilizing the same procedure given in Section 2.4 along with the relationship given in (67), we can rewrite the dynamic model of the robot manipulator in the following form:

$$M^*(q,Y)\ddot{e} + V_m^*(q,\dot{q},Y,\dot{Y})\dot{e} + N^*(q,\dot{q},Y,\dot{Y},\dot{Y}_d,\ddot{Y}_d) = T^{-T}\tau^* \tag{68}$$

where

$$M^*(q,Y) = T^{-T}C^{-T}M(q)C^{-1}T^{-1},$$

$$V_m^*(q,\dot{q},Y,\dot{Y}) = T^{-T}C^{-T}[M(q)(C^{-1}\dot{T}^{-1} + \dot{C}^{-1}T^{-1}) + V_m(q,\dot{q})C^{-1}T^{-1}],$$

$$N^*(q,\dot{q},Y,\dot{Y},\dot{Y}_d,\ddot{Y}_d) = -T^{-T}C^{-T}[M(q)C^{-1}T^{-1}\ddot{Y}_d + G(q) + F(\dot{q})] - T^{-T}C^{-T}[M(q)(C^{-1}\dot{T}^{-1} + \dot{C}^{-1}T^{-1}) + V_m(q,\dot{q})C^{-1}T^{-1}]\dot{Y}_d,$$

$$\tau^*(q,t) = -C^{-T}\tau.. \tag{69}$$

Based on the expression given in (68) and (69), we can now utilize the procedure given in Section 3.1 to develop the open-loop error system as follows:

$$M^*\dot{r} = -k_s r - V_m^* r + Y_r\tilde{\phi}_r + Y_r\hat{\phi}_r + k_s r + T^{-T}\tau^* \tag{70}$$

where the regression matrix parametrization $Y_r\phi_r$ is now defined as

$$Y_r\phi_r = \mu_r M^*\dot{e} + \mu_r V_m^* e - N^*. \tag{71}$$

5.3. Closed-Loop Error System

Based on the open-loop error system given in (70), we can now design the auxiliary control signal $\tau^*(t)$ as follows:

$$\begin{bmatrix} \tau_1^* \\ \tau_2^* \\ \tau_3^* \end{bmatrix} = \begin{bmatrix} -\hat{D}^{-1}\begin{bmatrix} (Y_r\hat{\phi}_r + k_s r)_1 \\ (Y_r\hat{\phi}_r + k_s r)_2 \end{bmatrix} \\ \dfrac{1}{Y_\gamma\hat{\phi}_\gamma}(Y_r\hat{\phi}_r + k_s r)_3 \end{bmatrix} \tag{72}$$

where the elements of the adaptive estimate matrix $\hat{D}(t)$, and the parameter estimate vectors $\hat{\phi}_\gamma(t)$, $\hat{\phi}_r(t)$, were defined in (42), (43), and (46), respectively, and the auxiliary signal $\Omega_1(t) \in \mathbb{R}^{p2}$ originally defined in (44) is redefined as follows:

$$\Omega_1 = -r_3\Gamma_5\frac{Y_\gamma^T}{Y_\gamma\hat{\phi}_\gamma}(Y_r\hat{\phi}_r + k_s r)_3. \tag{73}$$

After substituting (72) and (70) for $\tau^*(t)$, we can obtain the following closed-loop error system:

$$M^*\dot{r} = -k_s r - V_m^* r + Y_r\tilde{\phi}_r - \begin{bmatrix} \tilde{D}\hat{D}^{-1} & 0_{2\times 1} \\ 0_{1\times 2} & \dfrac{Y_\gamma\tilde{\phi}_\gamma}{Y_\gamma\hat{\phi}_\gamma} \end{bmatrix}(Y_r\hat{\phi}_r + k_s r). \tag{74}$$

Given the closed-loop error system in (74), it is now straightforward to utilize the same stability analysis arguments given in Section 4 to prove the following theorem.

Theorem 2: *Provided the assumptions given in Remark 2, Remark 3, and Remark 7 are valid with respect to the fixed-camera configuration, the control torque input given in (42)–(44), (46), and (72) ensures asymptotic camera-space position and orientation tracking, in the sense that*

$$\lim_{t\to\infty} e(t) = 0 \tag{75}$$

where $e(t)$ was defined in (62).

Proof: See the proof of Theorem 1.

6. SIMULATION RESULTS

The proposed camera-in-hand regulation controller was simulated for a planar, three-link robot manipulator with the following dynamic model:[21]

$$\begin{bmatrix} \tau_1 \\ \tau_2 \\ \tau_3 \end{bmatrix} = \begin{bmatrix} p_1 + 2p_3\cos(q_2) & p_2 + p_3\cos(q_2) & p_5 \\ p_2 + p_3\cos(q_2) & p_4 & p_5 \\ p_5 & p_5 & p_5 \end{bmatrix}\begin{bmatrix} \ddot{q}_1 \\ \ddot{q}_2 \\ \ddot{q}_3 \end{bmatrix} + \begin{bmatrix} -p_3\sin(q_2)\dot{q}_2 & -p_3\sin(q_2)(\dot{q}_1 + \dot{q}_2) & 0 \\ p_3\sin(q_2)\dot{q}_1 & 0 & 0 \\ 0 & 0 & 0 \end{bmatrix}\begin{bmatrix} \dot{q}_1 \\ \dot{q}_2 \\ \dot{q}_3 \end{bmatrix} \tag{76}$$

where $p_1 = 3.473$ kg m^2, $p_2 = 0.242$ kg m^2, $p_3 = 0.193$ kg m^2, $p_4 = 0.3$ kg m^2, and $p_5 = 0.2$ kg m^2. The desired setpoint was selected in the robot task-space as follows:

$$x_d = \begin{bmatrix} 0.2826 \text{ m} \\ 0.5937 \text{ m} \end{bmatrix}, \quad \theta_d = 45 \text{ deg}. \tag{77}$$

The camera parameters defined in (11) were selected as follows:

$$\alpha_1 = 27.31 \text{ pixel m}^{-1}, \quad \alpha_2 = 27.31 \text{ pixel m}^{-1},$$

$$\theta_0 = 30 \text{ deg}. \tag{78}$$

Note that the parameter values given above were only required to simulate the proposed controller, [i.e., the parameter values given in (78) are not required for the proposed adaptive controller]. The initial joint-space values for each link were selected as follows:

$$q_1(0) = 30 \text{ deg}, \quad q_2(0) = 30 \text{ deg}, \quad q_3(0) = 0.0 \text{ deg}. \tag{79}$$

The control and adaptation gains were tuned until the best response was obtained. The values for the gains are given below:

$$k_1 = 20.0, \quad k_3 = 20.0, \quad k_3 = 20.0, \quad \alpha = 0.15,$$

$$\Gamma_1 = 1.0, \quad \Gamma_2 = 1.0, \quad \Gamma_3 = 1.0, \quad \Gamma_4 = 1.0,$$

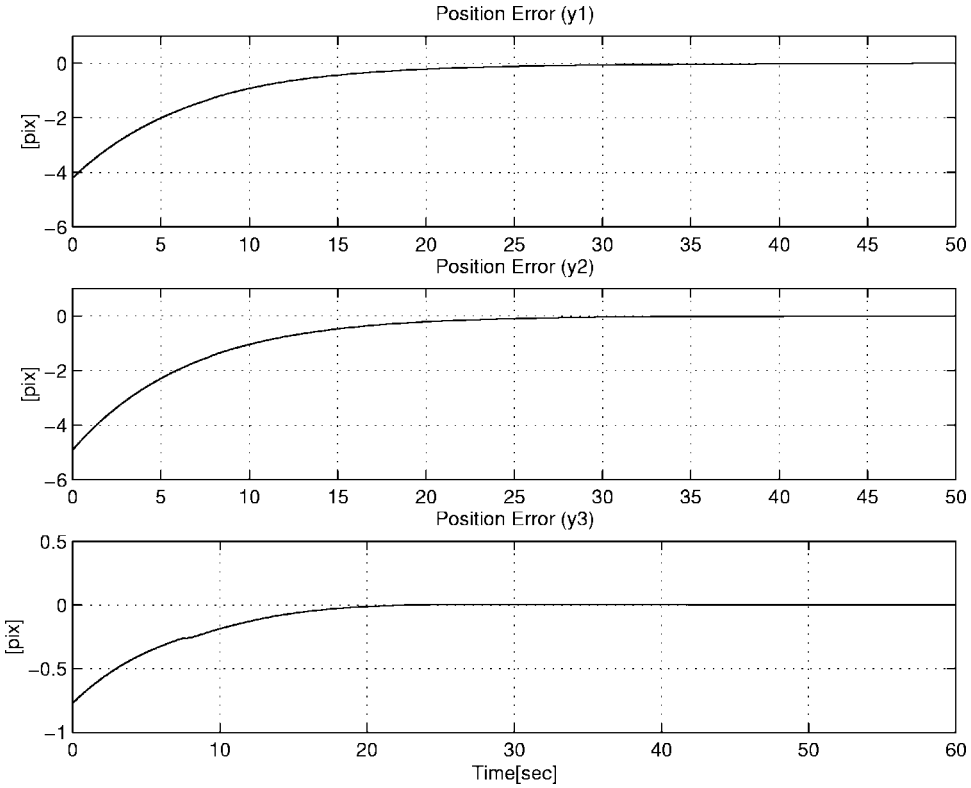

Figure 2. Camera-space position and orientation errors.

$$\Gamma_6 = \text{diag}\{2.0,2.0\},$$

$$\Gamma_7 = \text{diag}\{0.2,0.2,0.2,0.2,0.2,0.2,0.2,0.2,0.2,0.2,2.0,$$
$$2.0,0.2,2.0,2.0,2.0\}, \tag{80}$$

where each element of the estimate vectors $\hat{\phi}_r(t)$ and $\hat{\phi}_H(t)$ was initialized to 0.0, while the matrix $\hat{D}(t)$ was initialized to be nonsingular as follows:

$$\hat{D}(0) = \begin{bmatrix} 1.0 & 0 \\ 0 & 1.0 \end{bmatrix}. \tag{81}$$

The camera-space position and orientation tracking errors are shown in Figure 2 and the associated control torque inputs are shown in Figure 3. The parameter estimates for elements of the matrix D defined in (22) are shown in Figure 4. The plots for the parameter estimates of ϕ_r and ϕ_H are not shown for the sake of brevity.

Remark 8: For simplicity, we selected the camera parameters α_1, α_2 such that

$$\alpha_1 = \alpha_2. \tag{82}$$

Based on (82), the expression given in (30) is simplified to the following expression:

$$\frac{1}{\gamma} = \frac{1}{1+\theta_T^2} \tag{83}$$

and hence we did not need to adapt for ϕ_γ of (43) since the expression given in (83) is measurable.

7. CONCLUSION

In this paper, we have presented an asymptotic position and orientation controller for the camera-in-hand regulation problem. Specifically, we utilize an uncalibrated camera that is held by the end-effector of a robot manipulator with uncertain mechanical parameters to obtain the position and orientation of an object in the camera-space. We then regulate the camera-space position and orientation utilizing an adaptive controller that compensates for the uncer-

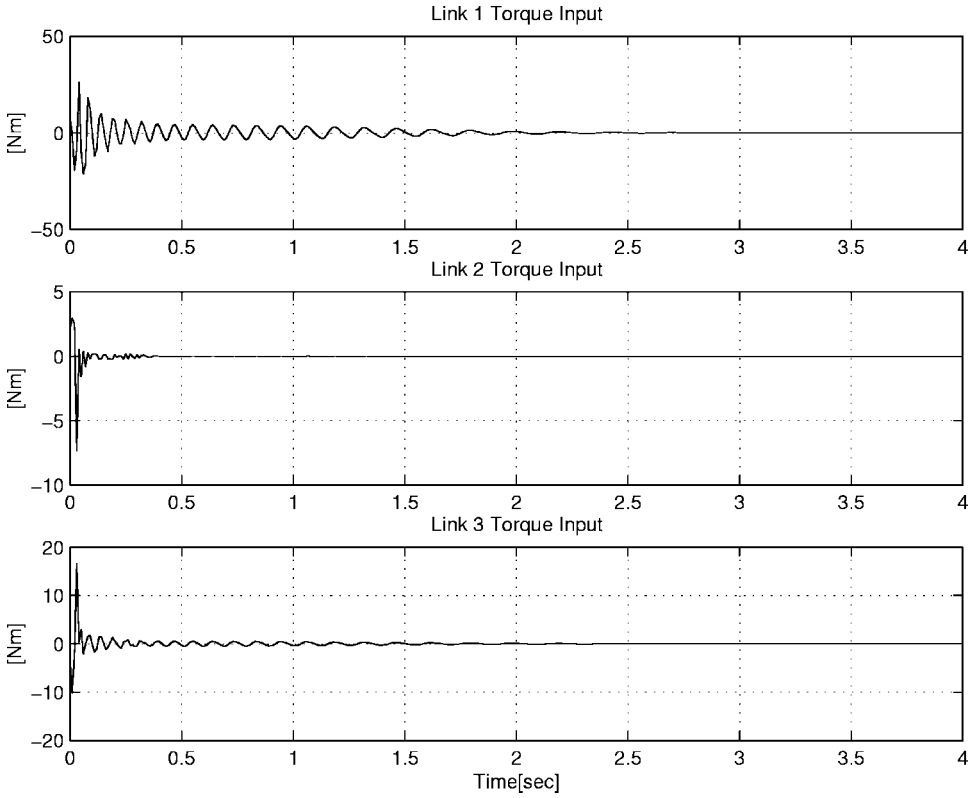

Figure 3. Control torque inputs.

tainty in the robot-camera system. An extension is also provided that illustrates how slight modifications can be made to the camera-in-hand configuration controller to achieve asymptotic position and orientation tracking for the fixed-camera configuration. Simulation results are provided to demonstrate the effectiveness of the camera-in-hand controller, and future work will concentrate on constructing an experimental testbed to further illustrate the effectiveness of the proposed controller. The testbed will consist of (i) an IMI direct drive robot manipulator, (ii) a Pentium II-based PC operating under QNX which will be utilized for implementing the control algorithms, and (iii) a Dalsa CAD-6 camera that is able to capture 955 frames per second with an eight-bit gray scale at a 256×256 resolution (i.e., a data rate of 63 megabytes per second).

8. APPENDIX A: EXPRESSION FOR CAMERA-SPACE ORIENTATION

To develop the expression given in (12), we first develop a relationship between the orientation of an object in the task-space and the position of two features of the object in the task space. Specifically, using basic geometrical observations (see Figure 5), we obtain the following expression:

$$\tan \theta_d = \left(\frac{x_{d22} - x_{d21}}{x_{d12} - x_{d11}} \right) \tag{A1}$$

where $\theta_d(t) \in \Re^1$ represents the desired orientation of the object in the task-space and $x_{d1j}, x_{d2j} \in \Re^1$ denote the desired position of the jth feature point in the task-space (see Figure 5). We then utilize the camera model given in (7) to express the position of the jth feature point in the camera-space as shown below:

$$\begin{bmatrix} y_{d1j}(t) \\ y_{d2j}(t) \end{bmatrix} = BR(\theta) \left(\begin{bmatrix} x_1(t) \\ x_2(t) \end{bmatrix} - \begin{bmatrix} x_{d1j} \\ x_{d2j} \end{bmatrix} \right), \quad \forall\, j = 1,2, \tag{A2}$$

where $y_{dj}(t), y_{dj}(t) \in \Re^1$ represent the position of the jth feature in the camera-space, B was defined in (8),

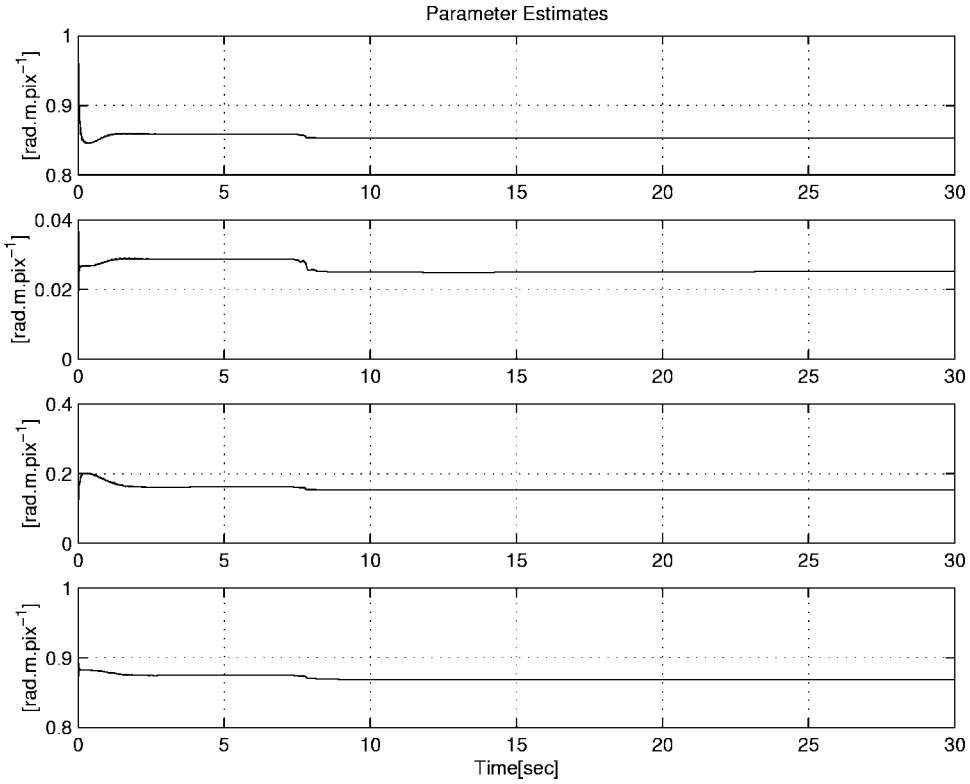

Figure 4. Parameter estimates for $D(t)$.

R was defined in (10), and $x_1(t), x_2(t) \in \Re^1$ represent the position of the end-effector in the task-space (see Figure 5). To obtain the camera-space orientation of the object, we now utilize the same geometrical observation utilized in (A1) to obtain the following expression:

$$\tan \theta_y = \left(\frac{y_{d22} - y_{d21}}{y_{d12} - y_{d11}} \right). \tag{A3}$$

After substituting the expressions given in (A2) for $y_{d1j}(t)$ and $y_{d2j}(t)$ $\forall j=1,2$ into (A3) and performing some algebraic manipulation, we can obtain the relationship between the task-space orientation and the camera-space orientation that is given in (12).

A similar procedure could be used for the fixed camera extension case, where the orientation of the end-effector can be obtained in camera space. This leads to the expression given in (63).

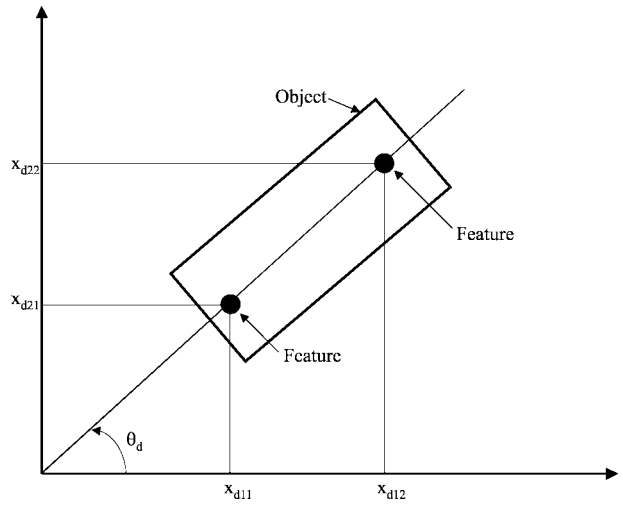

Figure 5. Geometric relationship between the position of object features and the object orientation in the task-space.

9. APPENDIX B: PROJECTION ALGORITHM

In order to show that the expression given in (54) reduces to the expression in given in (56), we substitute for the update laws given in (42), (45), and (46) and then cancel common terms to obtain the following expression:

$$\dot{V} \leq -k_s r^T r - r_3 \frac{Y_\gamma \tilde{\phi}_\gamma}{Y_\gamma \hat{\phi}_\gamma}[(Y_r \hat{\phi}_r + k_s r)_3 + Y_H \hat{\phi}_H] - \tilde{\phi}_\gamma^T \Gamma_5^{-1} \dot{\hat{\phi}}_\gamma. \quad \text{(B1)}$$

Now, if we substitute for the adaptation laws given in (43) and (44), then we must evaluate (B1) for each of the three cases given in (43). In addition to showing that (54) reduces to the expression given in (56), we will describe how the parameter update laws given in (43) and (44) ensure that if $\hat{\vartheta}_\gamma(0) \in \text{int}(\Lambda_1)$, then $\hat{\phi}_\gamma(t)$ never leaves the region Λ_1, $\forall t \geq 0$.

Case 1: $\hat{\phi}_\gamma(t) \in \text{int}(\Lambda_1)$.

When the estimate $\hat{\phi}_\gamma(t)$ lies in the interior of the convex region Λ_1, described in Property 4, (B1) can be expressed as

$$\dot{V} \leq -k_s r^T r - r_3 \frac{Y_\gamma \tilde{\phi}_\gamma}{Y_\gamma \hat{\phi}_\gamma}[(Y_r \hat{\phi}_r + k_s r)_3 + Y_H \hat{\phi}_H] + r_3 \tilde{\phi}_\gamma^T \frac{Y_\gamma^T}{Y_\gamma \hat{\phi}_\gamma}[(Y_r \hat{\phi}_r + k_s r)_3 + Y_H \hat{\phi}_H], \quad \text{(B2)}$$

thus, for Case 1, we can conclude that (54) reduces to the expression in given in (56). In addition, the direction in which the estimate $\hat{\phi}_\gamma(t)$ is updated for Case 1 is irrelevant, since the worse case scenario is that $\hat{\phi}_\gamma(t)$ will move toward the boundary of the convex region denoted by $\partial(\Lambda_1)$.

Case 2: $\hat{\phi}_\gamma(t) \in \partial(\Lambda_1)$ and $\Omega_1^T \hat{\phi}_\gamma^\perp \leq 0$.

When the estimate $\hat{\phi}_\gamma(t)$ lies on the boundary of the convex region Λ_1 described in Property 4 and $\Omega_1^T \hat{\phi}_\gamma^\perp \leq 0$ then (B1) can be expressed as (B2); thus, for Case 2, we can conclude that (54) reduces to the expression in given in (56). In addition, the vector Ω_1 has a zero or nonzero component perpendicular to the boundary $\partial(\Lambda_1)$ at $\hat{\phi}_\gamma$ that points in the direction toward the int(Λ_1). Geometrically, this means that $\hat{\phi}_\gamma$ is updated such that it either moves toward the int(Λ_1) or remains on the boundary; hence, $\hat{\phi}_\gamma(t)$ never leaves Λ_1.

Case 3: $\hat{\phi}_\gamma(t) \in \partial(\Lambda_1)$ and $\Omega_1^T \hat{\phi}_\gamma^\perp > 0$.

When the estimate $\hat{\phi}_\gamma(t)$ lies on the boundary of the convex region Λ_1 described in Property 4 and $\Omega_1^T \hat{\phi}_\gamma^\perp > 0$, then (B1) can be expressed as

$$\dot{V} \leq -k_s r^T r - \tilde{\phi}_\gamma^T \Gamma_5^{-1}[-\Omega_1 + P_r^t(\Omega_1)] \quad \text{(B3)}$$

where (44) was utilized. Based on (B3), we can utilize Property 4 to conclude that

$$\dot{V} \leq -k_s r^T r - \tilde{\phi}_\gamma^T \Gamma_5^{-1}\{-[P_r^\perp(\Omega_1) + P_r^t(\Omega_1)] + P_r^t(\Omega_1)\} \leq -k_s r^T r + \tilde{\phi}_\gamma^T \Gamma_5^{-1} P_r^\perp(\Omega_1). \quad \text{(B4)}$$

Because $\hat{\phi}_\gamma \in \partial(\Lambda_1)$, and $\hat{\phi}_\gamma$ must lie either on the boundary or in the interior of Λ_1, then the convexity of Λ_1 implies that $\tilde{\phi}_\gamma(t)$ defined in (49) will either point tangent to $\partial(\Lambda_1)$ or toward int(Λ_1) at $\hat{\phi}_\gamma(t)$. That is, $\hat{\phi}_\gamma(t)$ will have a component in the direction of $\hat{\phi}_\gamma^\perp(t)$ that is either zero or negative. In addition, since $P_r^\perp(\Omega_1)$ points away from int(Λ_1), we have that $\tilde{\phi}_\gamma^T \Gamma_5^{-1} P_r^\perp(\Omega_1) \leq 0$; thus, (B4) reduces to (56). Furthermore, since $\dot{\hat{\phi}}_\gamma(t) = P_r^t(\Omega_1)$, we are ensured that $\hat{\phi}_\gamma(t)$ is updated such that it moves tangent to $\partial(\Lambda_1)$; hence, $\hat{\phi}_\gamma(t)$ never leaves Λ_1.

ACKNOWLEDGMENTS

This work was supported in part by National Multiple Sclerosis Society PP1069 at Clarkson University, in part by AFOSR Contract No. F49620-03-1-0381 at the University of Florida, and in part by a DOC grant, an ARO Automotive Center grant, a DOE contract, a Honda Corporation grant, and a DARPA contract at Clemson University.

REFERENCES

1. R. Kelly, Robust asymptotically stable visual servoing of planar robots, IEEE Trans. Rob. Autom. 12:(5) (1996), 759–766.
2. G.D. Hager, W.C. Chang, and A.S. Morse, Robot hand-eye coordination based on stereo vision, IEEE Control Syst. Mag. 15:(1) (1995), 30–39.
3. F. Miyazaki and Y. Masutani, Robustness of sensory feedback control based on imperfect Jacobian, Robotics Research: The Fifth Int Symp, H. Miura and S. Arimoto (Editors), MIT Press, Cambridge, MA, 1990, pp. 201–208.
4. B.E. Bishop and M.W. Spong, Adaptive calibration and control of 2D monocular visual servo system, IFAC symp robot control, Nantes, France, 1997, pp. 525–530.
5. G.D. Hager and S. Hutchinson (Guest Editors), Special section on vision-based control of robot manipulators, IEEE Trans. Rob. Autom. 12:(5) (1996).
6. B. Nelson and N. Papanikolopoulos (Guest Editors),

Special issue of visual servoing, IEEE Rob. Autom. Mag. 5:(4) (1998).
7. R. Kelly and A. Marquez, Fixed-eye direct visual feedback control of planar robots, J. Syst. Eng. 4:(5) (1995), 239–248.
8. R. Kelly, F. Reyes, J. Moreno, and S. Hutchinson, A two-loops direct visual control of direct-drive planar robots with moving target, Proc IEEE Int Conf Rob Autom (1999), 599–604.
9. R. Kelly, R. Carelli, O. Nasisi, B. Kuchen, and F. Reyes, Stable visual servoing of camera-in-hand robotic systems, IEEE/ASME Trans. Mechatron. 5:(1) (2000), 39–48.
10. M. Takegaki and S. Arimoto, A new feedback method for dynamic control of manipulators, ASME J. Dyn. Syst., Meas., Control 103 (1981), 119–125.
11. A. Maruyama and M. Fujita, Robust visual servo control for planar manipulators with eye-in-hand configurations, Proc 36th IEEE Conf Decision Control (1997), 2551–2552.
12. E. Zergeroglu, D.M. Dawson, M.S. de Queiroz, and A. Behal, Vision-based nonlinear tracking controllers with uncertain robot-camera parameters, Proc IEEE/ASME Int Conf Advanced Methatronics (1999), 854–859.
13. E. Zergeroglu, D.M. Dawson, M. de Queiroz, and S. Nagarkatti, Robust visual-servo control of planar robot manipulators in the presence of uncertainty, Proc 38th IEEE Conf Decision Control (1999), 4137–4142.
14. W.E. Dixon, D.M. Dawson, E. Zergeroglu, and A. Behal, Adaptive tracking control of a wheeled mobile robot via an uncalibrated camera system, Proc Am Control Conf, Chicago (2000), 1493–1497.
15. M.W. Spong and M. Vidyasagar, Robot dynamics and control, John Wiley and Sons, Inc., New York, 1989.
16. F.L. Lewis, C.T. Abdallah, and D.M. Dawson, Control of robot manipulators, Macmillan Publishing Co., New York, 1993.
17. R. Lozano and B. Brogliato, Adaptive control of robot manipulators with flexible joints, IEEE Trans. Autom. Control 37 (1992), 174–181.
18. D.M. Dawson, J. Hu, and T.C. Burg, Nonlinear control of electric machinery, Marcel Dekker, New York, 1998.
19. J.J. Slotine and W. Li, Applied nonlinear control, Prentice Hall, Inc., Englewood Cliffs, NJ, 1991.
20. R.K. Lenz and R.Y. Tsai, Techniques for calibration of the scale factor and image center for high accuracy 3-D machine vision metrology, IEEE Trans. Pattern Anal. Mach. Intell. 10:(5) (1988).
21. Integrated Motion, Inc., Direct drive manipulator research and development package operations manual, Berkeley, CA, 1992.